

## Fractal strain distribution and its implications for cross-section balancing

SCHUMAN WU

CogniSeis Development, Inc., 4775 Walnut Street, Suite 2A, Boulder, CO 80301, U.S.A.

(Received 24 September 1991; accepted in revised form 13 November 1992)

**Abstract**—Rock units having different physical properties show contrasts in structural styles. Massive competent rocks have relatively simple geometry and control the structural framework, whereas thin-bedded, less competent units are characterized by complex deformation at smaller scales. These contrasting structural styles can be quantified by a fractal dimension  $D$ . A fold profile with a  $D$  close to 1 has a simple geometry. A value of  $2 > D > 1$  indicates a fractal profile. A fractal profile has a fractal strain distribution such that the measured shortening increases with resolution. For rock units having different values of  $D$ , the shortening strains measured with the same resolution cannot be compared because a significant amount of deformation takes place at smaller scales for these units with a larger  $D$ . Proper balancing requires high-resolution analysis for these units to resolve strain at smaller scales.

In the central Appalachians, West Virginia, the Cacapon Mountain anticlinorium has a large ramp anticline in Cambrian–Ordovician rocks, which has a net shortening of 10.510 km as measured by section restoration. In contrast, restoration of the overlying complexly folded and faulted Upper Ordovician through Devonian units indicated a 3.660-km shortening. Thin section analysis revealed a 15–20% strain, equivalent to another 3-km shortening, and the remaining difference in shortening between the cover and the underlying blind thrust sheet has been previously attributed to forethrusting. Fractal analysis indicates that the Cambrian–Ordovician thrust sheet has a  $D = 1.001$  and the cover fold profile has a  $D = 1.072$ , which indicates a fractal geometry. If thin section scale through outcrop scale to map scale strains are included in the cross-section balancing, the cover sequence has a comparable shortening to that in the underlying thrust sheet.

### INTRODUCTION

DETERMINATION of the total shortening across a fold-thrust belt is important in order to quantify the deformation. However, estimates of shortening in different lithological units are often different, suggesting either the section cannot be balanced or that the method of estimation is inadequate. Problematic sections are likely where the geological data are not very reliable, as is generally the case for reconnaissance data covering a large area. However, detailed data from large-scale geologic maps covering small areas are relatively reliable and problematic sections are less likely, depending on the amount of subsurface geologic information available for section construction. In this paper, a large-scale geologic map and the accompanying section are used to illustrate a fractal strain distribution. The study indicates that a higher resolution structural analysis is necessary for rock units having a larger fractal dimension in order to determine the total shortening and balance the section.

The fractal nature of some geological features was described by geologists long before Mandelbrot (1967, 1983) invented the fractal theory. For example, the familiar anticlinorium and synclinorium are fractal patterns (Fig. 1). In the field, the so-called 'S', 'Z', 'M' and 'W' parasitic folds are observable from different parts of some outcrop-scale folds. In thin sections of low-grade schist, crenulations are common. Even within individual grains of some common rock minerals, kink bands, undulatory extinction and twins indicate distortion and bending of the crystal lattice. This scaling property of the entire series of deformation features ranging from tens

of kilometers to microns in scale indicates a fractal geometry. For profile b in Fig. 1, part of the anticlinorium or synclinorium can be enlarged by a certain factor to resemble the whole profile. Profile c in Fig. 1 also has this scaling property, except that the magnification factor in the vertical direction should be different from that in the horizontal direction. In fractal terminology, it can be stated that the Hausdorff–Besicovitch dimensions  $D$  (Mandelbrot 1983) of the profiles b and c in Fig. 1 are larger than their topological dimensions (such that a simplistic profile has a topological dimension of 1). Recognition of this fractal geometry is very important to structural geologists, because  $D$  indicates a fractal strain distribution and quantifies how the estimated shortening increases with the resolution of structural analysis.

To illustrate this scaling property of total shortening of folded rocks, the Cacapon Mountain anticlinorium (Fig. 2) in the central Appalachian Valley and Ridge province was selected as a field example because abundant geological and geophysical data and reliable cross-sections are available (Geiser 1974, Jacobeen & Kanes 1974, Perry 1978, Dean *et al.* 1985, Kulander & Dean 1986, Mitra 1986, 1987, Wilson & Shumaker 1988, Ferrill & Dunne 1989). Specifically, the cross-section (1:48,000) accompanying the large-scale (1:24,000) geologic map in the Cacapon Mountain area published by Dean *et al.* (1985) provides an excellent fold profile for Fourier and fractal analysis. The central Appalachian structural style varies in two different litho-tectonic packages (Fig. 3). In the Cambrian–Ordovician (CO) carbonates, ramps which connect a lower décollement in the Lower Cambrian Waynesboro Formation and an upper décollement in the Upper Ordovician Martins-

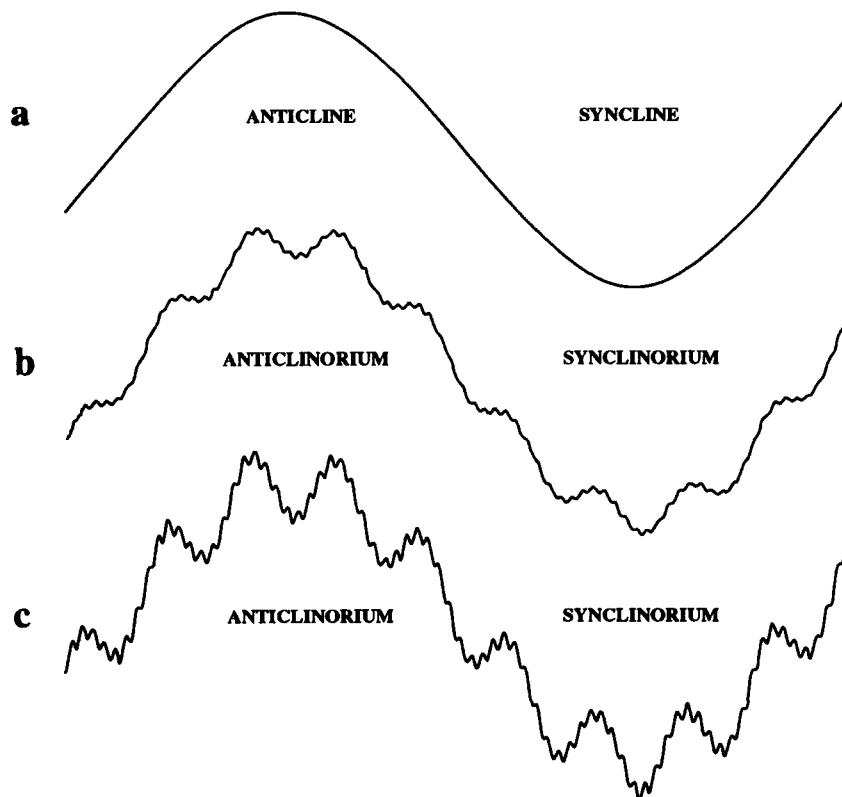


Fig. 1. Simple fold profile and fractal fold profiles. The anticlinorium and synclinorium are formed by superimposing smaller scale folds. Profile b is a self-similar fractal since folds at each level have a constant amplitude to wavelength ( $a/w$ ) ratio. Profile c is a self-affine fractal in which the  $a/w$  ratio of folds at each smaller scale is doubled (smaller folds can also have reduced  $a/w$  ratio).

burg Formation have produced large-scale ramp anticlines or blind duplexes (Jacobeen & Kanies 1974, Perry 1978, Dean *et al.* 1985, Kulander & Dean 1986, Mitra 1986, 1987, Geiser 1988, Wilson & Shumaker 1988, Ferrill & Dunne 1989). The overlying Upper Ordovician, through Mississippian, predominantly clastic sequences, on the other hand, are complexly folded with abundant small-scale thrust faults. This is nicely illustrated by the Cacapon Mountain anticlinorium (Fig. 4), where folds of various wavelengths with small thrust faults in the Upper Ordovician, Silurian, and Devonian sequence overlie a large blind ramp anticline in the Cambrian–Ordovician carbonates.

Although the available geologic data are detailed and reliable, a problem occurs when one tries a bed-length restoration of such a ramp anticline and the overlying folded cover sequence (Ferrill & Dunne 1989). In order to determine the shortening across the Cacapon Mountain anticlinorium, the cross-section has been digitized and restored (Fig. 5) using GEOSEC™, a proprietary software from CogniSeis Development for cross-section construction, modeling, restoration and balancing. In the deformed state section (Fig. 4) the western reference line (west boundary of Fig. 4) is near the hinge of Sideling Hill syncline. The eastern reference (or loose line of Geiser 1988) is in the hinge of the Timber Ridge syncline above the Martinsburg décollement and on the E-dipping backlimb of the Cacapon Mountain anticlinorium beneath the Martinsburg décollement. The lower part of the reference line is nearly perpendicular

to bedding in the deformed state and restored to vertical in the restored state, indicating that there is a slight backward shear in the Cambrian–Ordovician carbonate units of the blind ramp anticline. Above the Martinsburg décollement, the reference line is currently inclined toward the west and restores to vertical in the undeformed state. This is a reasonable geometry which indicates a forward shear in the transport direction during deformation.

It is interesting to note that there is only about a 1.2 km shortening discrepancy between the Ordovician Oswego and Martinsburg Formations (Oo and Om in Figs. 4 and 5) and the Cambrian–Ordovician carbonates. This shortening discrepancy can be easily explained by a strain in the Oswego and Martinsburg Formations that is larger than that in the Cambrian–Ordovician carbonates. However, there is 7.43-km shortening discrepancy between the Silurian and Devonian units and the Cambrian–Ordovician carbonates (Fig. 5). Ferrill & Dunne (1989) determined that layer-parallel shortening caused by pressure solution in the cover sequence is about 15–20%. This gives 3.0–3.5 km net shortening. Assuming small-scale strain is zero (this may not be true as will be discussed later), there remains a 3.5–4.0 km difference in shortening between the cover and the underlying blind thrust sheet. Ferrill & Dunne (1989) attributed this difference in shortening to forethrusting, because no evidence suggests backthrusting. However, if all major blind thrust sheets in the Valley and Ridge province have forethrusting of several kilometers, the

accumulated shortening in the Appalachian plateau (where folds are superficial above an Ordovician and Silurian detachment; Rogers 1963, Gwinn 1964) will exceed tens or even hundreds of kilometers. This shortening, however, is not evident in the Appalachian plateau (Geiser 1988). Including small-scale strain data from thin section analysis is important in cross-section balancing (Woodward *et al.* 1986, Geiser 1988), but it is not enough if the total shortening has a fractal distribution because thin-section strain only measures the strain at millimeter to centimeter scale. Significant amounts of shortening may also exist between centimeter and map scale.

### FRACTALS AND FRACTAL GEOMETRY OF FOLDED ROCKS

A fractal profile is defined by Mandelbrot (1983) as a curve with a Hausdorff–Besicovitch dimension ( $D$ ) greater than its topological dimension. A topological dimension is an integer such that a discrete point has a topological dimension of zero, a curve of 1, and so on. A fractal dimension of a profile describes how much of the two-dimensional plane it fills. If a profile is a simple curve without small-scale structures (such as the first profile in Fig. 1), its fractal dimension  $D = 1$ . If a curve is so complicated that it fills the entire plane, it has a fractal

dimension  $D = 2$ . Thus, a fractal profile has a fractal dimension  $1 < D < 2$  (such as the profiles b and c in Fig. 1).

There are two basic types of fractals: one is self-similar, the other is self-affine (Mandelbrot 1983, 1985), and both are statistically defined (Power & Tullis 1991). A self-similar fractal has a universal self-similarity which does not change with scale. When part of a self-similar fractal profile is magnified isotropically, it appears statistically the same as the entire profile. Profile b in Fig. 1 is a self-similar fractal, because folds in all scales were generated to have a constant amplitude-to-wavelength ratio. In a self-affine fractal profile, however, variable magnification factors have to be applied to an enlarged portion in order to resemble the entire profile (such as c in Fig. 1). An important aspect of a self-affine fractal is that the self-similarity is not universal and changes with scale (Mandelbrot 1985). In a two-dimensional Euclidean plane, a self-similar profile can be treated as a special case of self-affine fractal. Hence a self-affine model is more general and appears to be more appropriate for describing the geometry of folded rocks.

Examination of the cross-section in Fig. 4 reveals an interesting structural geometry. The ramp anticline in the blind Cambrian–Ordovician carbonate thrust sheet has a very simple fold profile. It has no small-scale structures, at least at the map resolution (1 mm in the original section represents 48 m). On the other hand, the

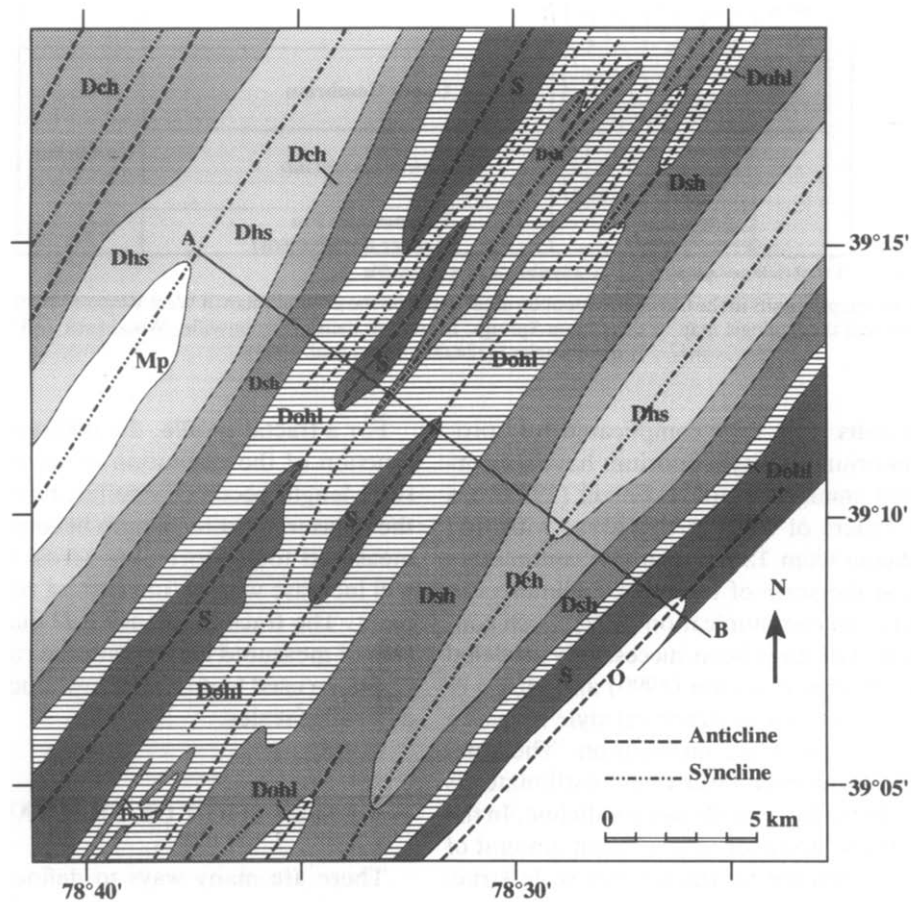
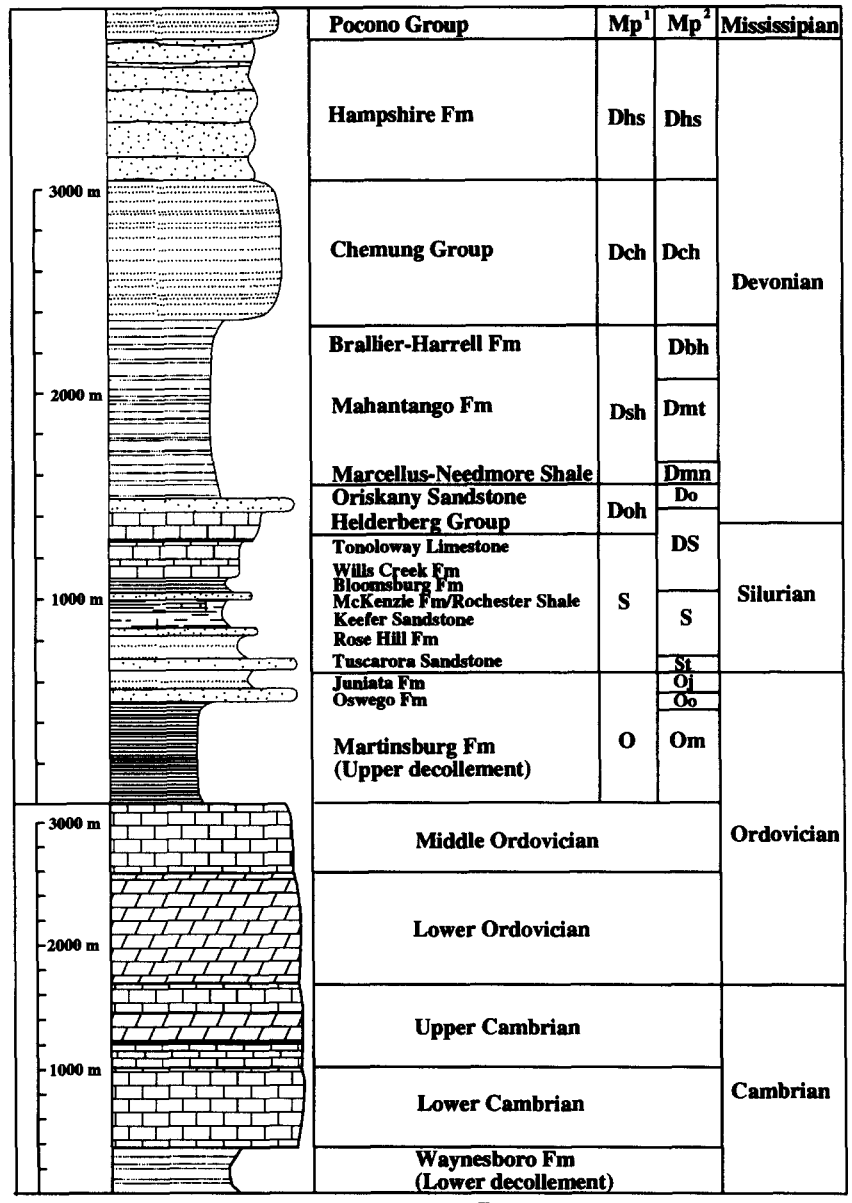


Fig. 2. Geologic map of Cacapon Mountain area. Geology is based on the geologic map of West Virginia (1:250,000; Cardwell *et al.* 1968) and the geologic map of the Capon Springs, Mountain Falls, Wardensville, Woodstock and Yellow Springs quadrangles (1:24,000; Dean *et al.* 1985). Stratigraphic abbreviations are explained in Fig. 3.



1 Symbols in geologic map (Fig. 2); 2 Symbols in cross section (Fig. 4).

Fig. 3. Stratigraphic units in the Cacapon Mountain area, based on the geologic map of West Virginia (1:250,000; Cardwell *et al.* 1968) and the geologic map of the Capon Springs, Mountain Falls, Wardensville, Woodstock and Yellow Springs quadrangles (1:24,000; Dean *et al.* 1985).

overlying cover units have very complicated fold profiles. The anticlinorium and synclinorium have numerous superimposed small-scale folds. Ferrill (1987) has recognized five orders of folds in this area, with fold wavelengths ranging from 12 km to a few centimeters plus microfolds at the scale of tenths of millimeters in shale (Ferrill personal communication 1992). Such contrasts in structural style have been successfully modeled in the laboratory by Liu & Dixon (1990) and Dixon & Tirrul (1991). This contrast in structural style reveals a significant difference in strain distribution. The total shortening of the Cambrian–Ordovician carbonates is well represented by the large-scale ramp anticline. In the overlying cover units, however, a significant amount of deformation is contributed by the smaller scale structures. In terms of fractal theory, the Cambrian–Ordovician carbonates have a small fractal dimension, and the cover has a larger fractal dimension.

For a fractal profile, the measured profile length is a function of the resolution of measurement. When the ruler length becomes smaller, resolution increases and the measured profile length becomes longer. Hence the measured total shortening across a fractal fold profile will increase with an increase of resolution of measurement. The fractal dimension *D* quantifies the changing rate of measured length with the ruler length, therefore *D* can be used to describe how much deformation exists at smaller scales.

**ESTIMATION OF FRACTAL DIMENSION**

There are many ways to define a fractal dimension (Mandelbrot 1983, 1985, Falconer 1990), such as compass dimension, box counting dimension, mass dimension and spectral dimension. According to Mandelbrot

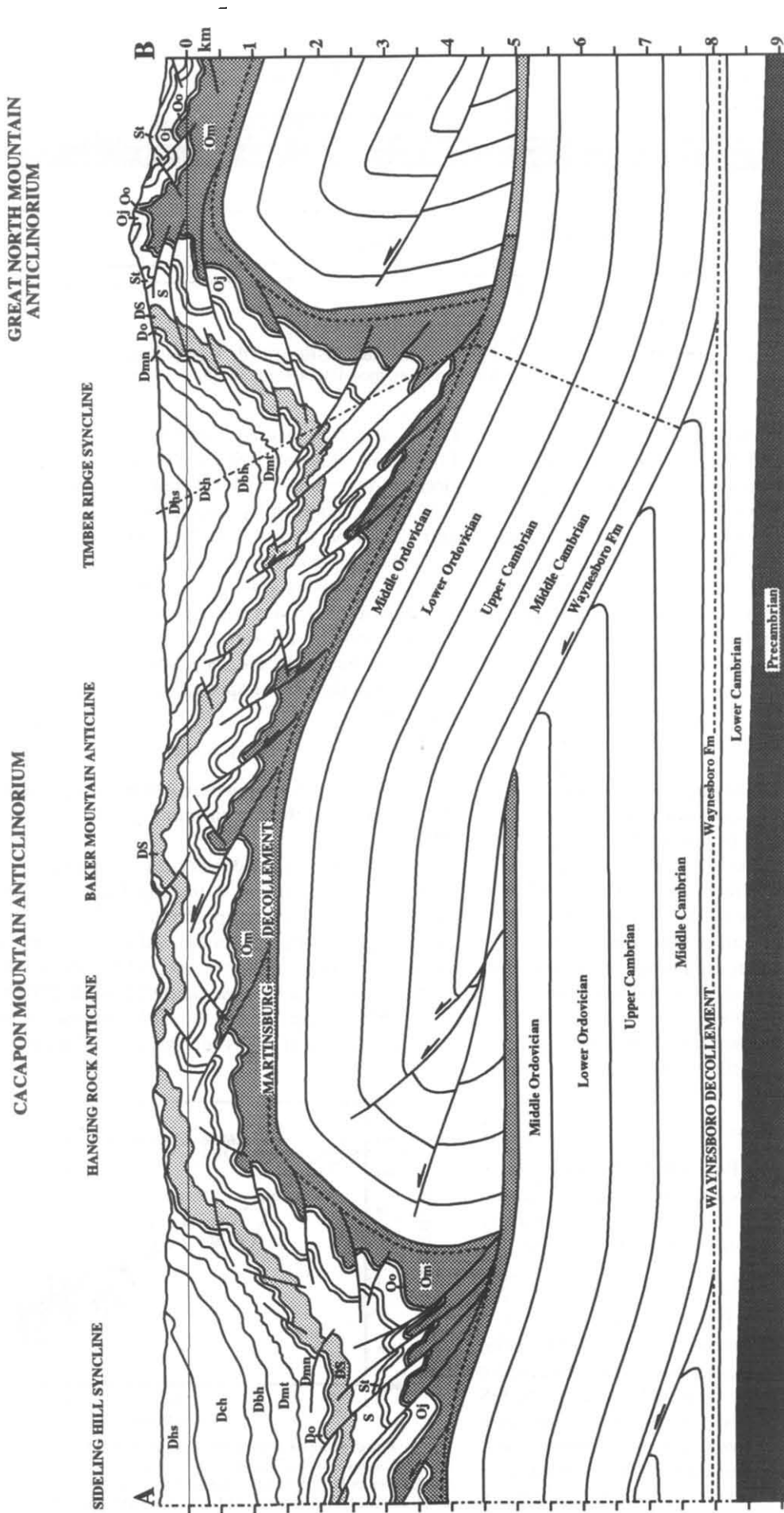


Fig. 4. Geologic cross-section across the Cacapon Mountain anticlinorium (from Dean *et al.* 1985). Location is shown in Fig. 2.

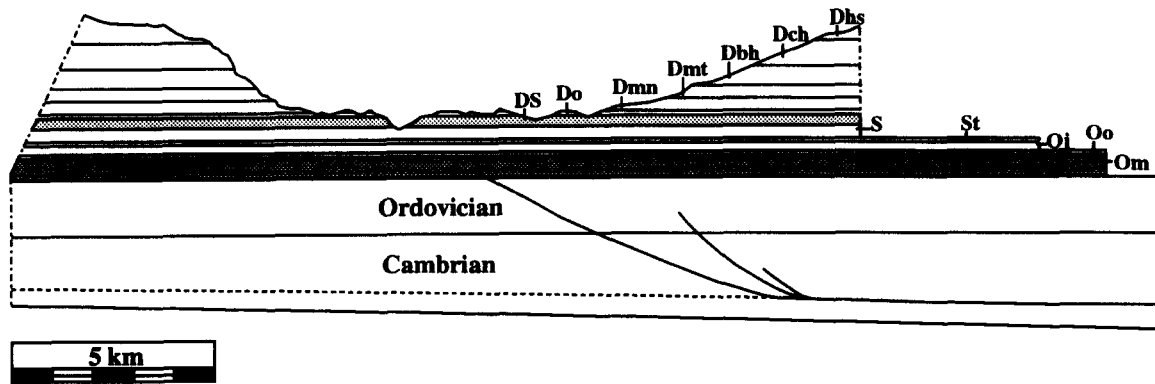


Fig. 5. Restored section across the Cacapon Mountain anticlinorium using GEOSEC<sup>TM</sup>, a proprietary software of CogniSeis Development, Inc. for cross-section construction, modeling, restoration and balancing.

(1985) the values yielded by these dimensions are identical only for a self-similar fractal. Caution must be taken when applying these methods to self-affine fractals. Not only do they yield different values but some methods are invalid. The fractal dimension may only apply to a certain range, because there is no universal  $D$  applying to all scales for a self-affine fractal. The fractal dimension of the Cacapon Mountain anticlinorium will be studied by a spectral method and a compass method. The limits of application of both methods are discussed and their results are compared.

#### Spectral method

Fourier analysis of a structural profile (which is called a spatial domain) provides the information about distribution of fold wavelength (or frequency, which is the reciprocal of wavelength) and amplitude in a wavelength (or frequency) domain (Wilson 1988). Fold amplitude and wavelength are directly related to the shortening of folded rocks. Their distribution is related to the strain distribution (the term strain used in this paper refers to the total shortening strain of a profile, which includes, but is not equal to, the internal strain). The Fourier transform can be used to estimate the power spectral density function  $G(k)$  (Chatfield 1984, Jenkins & Watts 1968) which has the form

$$G(k) = Ck^{-a} \quad (1)$$

(Brown 1987, Hough 1989, Power & Tullis 1991), where  $k$  is the wave number,  $C$  is a constant, and  $a$  is in the range of  $-2$  to  $-3$ . From the power spectral density function, the fractal dimension can be estimated by

$$D = (5 - a)/2 \quad (2)$$

(Brown 1987, Hough 1989, Power & Tullis 1991).

A discrete Fourier transform requires that the spatial function be single valued, i.e. for an  $x$  co-ordinate, there is only one corresponding  $y$  value. The base of the DS units in Fig. 4 was selected for a Fourier transform because it has representative cover unit structures and has limited faults and overturned folds. DS units (Fig. 3) contain the Devonian Helderberg Group (limestone), Silurian Tonoloway Limestone, Wills Creek Formation

(shale and thin bedded limestone) and Bloomsburg Formation (claystone with shale and thin-bedded limestone). According to Dean (personal communication 1992), the Bloomsburg Formation is intensely folded and cannot be shown on sufficiently small scale on the cross-section, and it is expected that fractal analysis can predict the missing amount of shortening.

The base of DS was digitized at a 0.1 inch (2.54 mm) interval and the Fourier coefficients ( $A$  and  $B$ ) were calculated by a FORTRAN program. From the Fourier coefficients the power spectral density function is estimated by

$$G(k) = NR_k^2/4\pi \quad (3)$$

(Chatfield 1984, p.135), where  $N$  is the sample size,  $R_k$  is the amplitude of the  $k$ th harmonic given by  $R_k^2 = Ak^2 + Bk^2$ .

The power spectral density function  $G(k)$  vs wave-number is plotted in Fig. 6 on a log-log scale. The slope of the best-fit line of the spectrum is 2.79. The spectrum of a self-similar fractal profile will have a slope of 2; a spectrum of a self-affine fractal profile will have a slope in the range  $1 < a < 3$ , excluding 2 (Fox & Hayes 1985, Fox 1989). Apparently the fold geometry in the Silurian-Devonian rocks indicates a self-affine fractal.

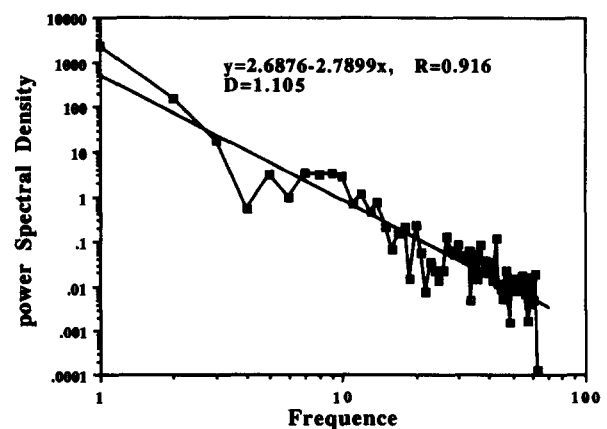


Fig. 6. Power spectral density function of the profile of the base of the DS (combined Silurian Wills Creek Formation, Tonoloway Limestone and Devonian Helderberg Group) in Fig. 4. The regression relation is obtained from the log-log scaled data. From the slope of the regression line, a fractal dimension of the DS profile is estimated as  $D = 1.105$ .

From the slope of the regression line, the fractal dimension is calculated as  $D = 1.105$  by using equation (2). The fractal dimension of the Cambrian–Ordovician rocks in Fig. 4 cannot be estimated by the spectral method because the fold profile is not single valued.

### Compass method

A compass method (Mandelbrot 1983) is more straightforward for determining the fractal dimension than the spectral method. By using a compass with a certain opening  $r$  (or a ruler of length  $r$ ) measuring along a profile, the fold arc length ( $L_o$ ) is measured.  $L_o(r)$  or the normalized arc length  $L_o(r)/L$ , where  $L$  is deformed length, tends to increase with increase of resolution (by reducing the ruler length  $r$ ).  $L_o(r)/L$  is used because this ratio is the reciprocal of stretch ( $S$ ). Plotted on a log–log graph,  $L_o(r)/L$  vs  $r$  will fall on a straight line statistically if the profile is a fractal. The relation between the fractal dimension  $D$  and  $L_o(r)/L$  is given by

$$L_o(r)/L = Ar^{(1-D)} \quad (4)$$

(Mandelbrot 1983, Okubo & Aki 1987, Power & Tullis 1991, Turcotte 1991), where  $A$  is a constant.

As discussed by Aviles *et al.* (1987), equation (4) implicitly requires that a compass begin and end at the specified end points. In practice, this is not possible, and the way of handling the remainder is very important. Three possibilities are discussed by Aviles *et al.* (1987). The first method is to take only those rulers that give a remainder less than a specified value or tolerance. The second method is to add the straight line distance between the ruler and the end of curve to the total length. A third method is to round up the straight line remainder. The tolerance method is used here as it has been proved by Aviles *et al.* (1987) to give the smallest scatter in a data set.

Both the DS and Cambrian–Ordovician units in Fig. 4 are measured by the compass method (Fig. 7). The fractal dimension of Cambrian–Ordovician rocks is very

close to 1 ( $D = 1.001$ ). This seems to make sense, because the Cambrian–Ordovician rocks do not appear to have a fractal geometry, e.g. there is no self similarity between small scale and large scale (no scaling property). However the  $D$  of 1.043 in the DS units seems to be underestimated, because of the apparent scaling property and the fact that a fractal dimension of 1.105 was obtained by the spectral method.

For a self-affine fractal, a compass may not give the right estimation of  $D$  as discussed by Mandelbrot (1985). There is a cross-over length  $b$  (Wong *et al.* 1986, Brown 1987, Power & Tullis 1991) such that if  $r \gg b$ , the curve appears to be smooth ( $D$  is close to 1) and, if  $r \ll b$ , the curve appears to be fractal. To use a compass method to estimate  $D$ , the resolution must satisfy  $r \ll b$ . The cross-over length  $b$  is implicitly defined by

$$\sigma = b(r/b)^{(2-D)} \quad (5)$$

(Brown 1987, Wong 1987), where  $\sigma$  is the standard deviation. When  $r = b$  then  $\sigma = b$ , which means that when a ruler with the cross-over length  $b$  is used, the standard deviation of the curve equals the value of  $b$ . The cross-over length  $b$  can be estimated from the power spectral density function by

$$G(k) = (4 - 2D)b^{(2D-2)}(k)^{-(5-2D)} \quad (6)$$

(Brown 1987).

From the power spectral function (Fig. 6), the cross-over length of the DS units in the profile (Fig. 4) is estimated to be  $b = 0.78$  mm. The minimum ruler used is 1 mm (Fig. 4), and therefore the value of the fractal dimension  $D$  in the DS units (Fig. 4) is underestimated.

It is still possible to use the compass method for estimating the fractal dimension by introducing a vertical exaggeration (Mandelbrot 1985, Brown 1987). A vertical-exaggeration factor needs to be determined first. The maximum ruler length (opening of the compass) used in this study is 40 mm, to make  $r$  small enough in comparison with  $b$ , and let  $r < 0.1b$ .  $D = 1.105$  (Fig. 6). Equation (5) becomes

$$\sigma = r^{0.895}b^{0.105}. \quad (7)$$

The standard deviation of the original profile is  $\sigma_o = 40^{0.895} 0.78^{0.105} = 26.45$ . To let  $r < 0.1b$  requires  $\sigma_r = 40^{0.895} (10 \times 40)^{0.105} = 50.94$ ; then the profile must be enlarged at least by a factor of 2 (as indicated by  $\sigma_r/\sigma_o$ ) in the vertical direction. To find the best vertical exaggeration, the DS profile in Fig. 4 has been exaggerated 2, 5, 10 and 20 times in the vertical direction. The results are shown in Fig. 8. Vertical exaggerations of  $\times 5$  and  $\times 10$  resulted in similar  $D$  values ( $D = 1.070$  and  $1.074$ , respectively). A  $D$  of 1.072 (the average of the two values) is used as the compass fractal dimension for the DS fold profile.

The compass  $D$  (1.072) after vertical exaggeration is still smaller than the spectral  $D$  (1.105). This may be an inherent difference between these two methods. It is not known at this time whether other techniques can be used to bring the two methods into closer agreement.

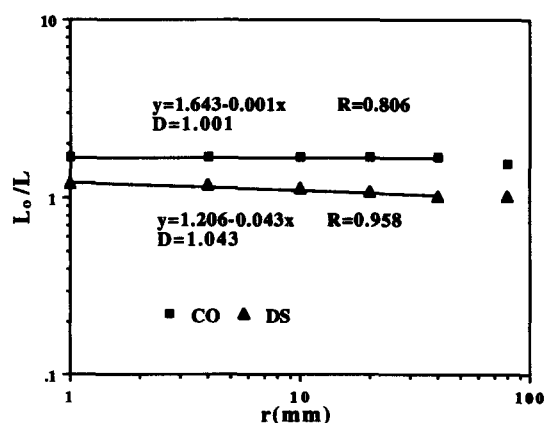


Fig. 7. Plot of  $L_o/L$  vs  $r$  for both CO (Cambrian–Ordovician) and DS profiles in Fig. 4. The compass fractal dimensions are estimated to be  $D = 1.001$  in CO and  $D = 1.043$  in DS.

**FRACTAL STRAIN DISTRIBUTION**

The ratio  $L_o(r)/L$  in Figs. 6–8 actually indicates a strain distribution.  $L_o/L$  is the reciprocal of stretch ( $S$ ), and can be converted into strain by  $L/L_o - 1$ . The shortening strain is plotted at the right side of Fig. 9 (log–log scale). Although the cross-section digitized in GEOSEC™ can be set to have a very high resolution (such as 0.5 m), the real resolution is limited by the scale of the geological cross-section. Under normal circumstances, we would not be able to recognize or draw structures less than about 1 mm. For the cross-section used here, 1 mm represents 48 m in real scale. As indicated in Fig. 9, at this resolution the shortening is about 40% in the Cambrian–Ordovician rocks and about 15% in the DS units.

As revealed by the fractal dimension  $D$ , however, the strain shows a fractal distribution. The Cambrian–Ordovician units have a small  $D$  which is almost equal to 1. It means that not much deformation has occurred on smaller scales. With an increase in the resolution of structural detail through mesoscopic and microscopic strain analysis, there likely will not be significant additional total shortening of the profile. On the other hand, the folded Upper Ordovician through Devonian units overlying the Cambrian–Ordovician carbonate rocks have a fractal dimension of 1.072 which means that a significant amount of deformation has occurred at smaller scales. With an increase in the resolution of structural detail, significant new data may be revealed about the total shortening of the fold profile.

In Fig. 9, the compass fractal dimension  $D$  of both DS and the Cambrian–Ordovician units has been extrapolated toward finer scales. The intersection point  $r_1$  ( $6.17 \times 10^{-7}$  m in map and about 0.030 m in real scale) represents the required resolution of structural analysis in order to estimate the total shortening in the DS units in which a  $D = 1.043$  is used. However, the compass  $D$  without treatment is underestimated for a self-affine fractal. The compass  $D$  with vertical exaggeration is also plotted in Fig. 9 using the cross-over length estimated

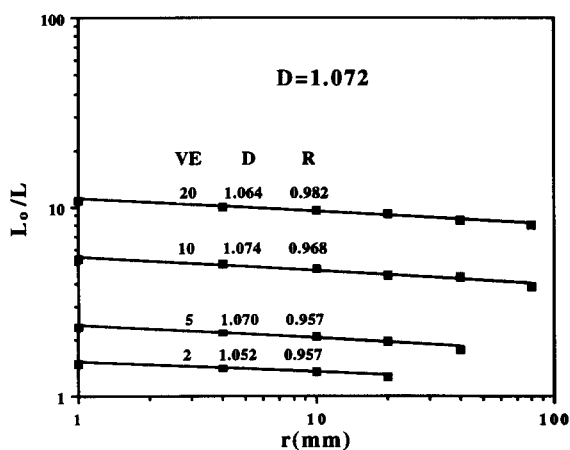


Fig. 8. Plot of  $L_o/L$  vs  $r$  for the DS profile after vertical exaggeration by factors of 2, 5, 10 and 20. The profiles vertically exaggerated  $\times 5$  and  $\times 10$  give similar results. An average fractal dimension is determined from these two results to be  $D = 1.072$ .

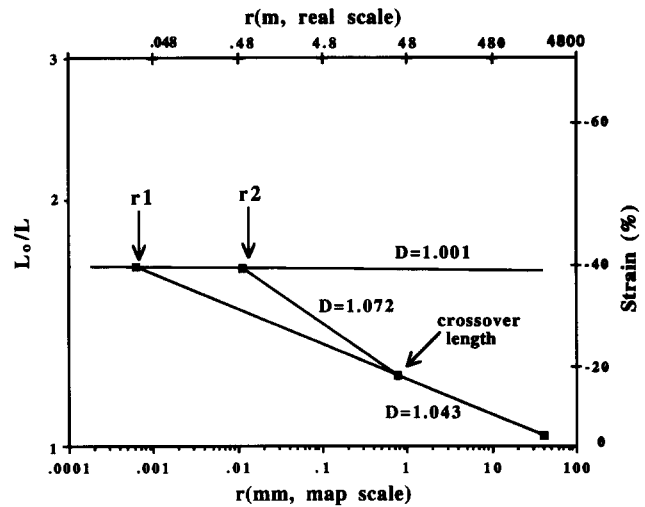


Fig. 9. Fractal strain distribution. The  $L_o/L$  ratios are converted into strain and indicated on the right. The fractal dimension of  $D = 1.001$  in the Cambrian–Ordovician units and the fractal dimensions of  $D = 1.043$  (without vertical exaggeration treatment) and  $D = 1.072$  (with vertical exaggeration treatment) in the Devonian–Silurian units are extrapolated toward the smaller scale. The range between the intersection points  $r_1$  and  $r_2$  indicates a minimum required resolution for balancing the total shortening in DS with the shortening in CO (see text for details).

from spectral analysis. The second intersection point  $r_2$  ( $11.6 \times 10^{-7}$  m in map and about 0.556 m in real scale) indicates the resolution of structural analysis required in order to balance the shortening in the DS units by using a  $D = 1.072$ . Although the exact positions of the intersection points depend on many uncertainties, such as the precision of the cross-section and a correct estimation of  $D$ , a structural analysis with a resolution ranging from cm to dm is required to determine the total shortening in the DS units (Fig. 9). As mentioned previously, the Bloomsburg Formation (at base of DS in Fig. 4) is more intensely folded than can be shown on the cross-section (Dean personal communication 1992). The relatively simple structures illustrated on the cross-section do not accurately represent the net shortening accommodated by folding and faulting. Both fractal analysis and field data suggest that structural analysis of higher resolution is necessary.

Ferrill & Dunne (1989) determined the thin section strain in the Silurian through Devonian units to be 15–20% which gives about 3–3.5 km net shortening at this scale (mm). However, strain is also distributed between the thin section scale (mm) and map scale (around 50 m in this case). At least five orders of folds have been recognized in the Cacapon Mountain area (Geiser 1974, Dean *et al.* 1985, Ferrill 1987). The fifth-order folds have wavelengths ranging from a few centimeters to meters (Fig. 10), and the fourth-order folds have wavelengths from a few meters to tens of meters (Geiser 1974, Dean *et al.* 1985, Ferrill 1987). Both fifth- and fourth-order folds are beyond the resolution of the cross-section at 1:48,000 scale, but as predicted in Fig. 9, the shortening produced by structures in this scale range is estimated to be about 10% (Fig. 10). If strains from the entire scale range are included in the section balancing, the cover



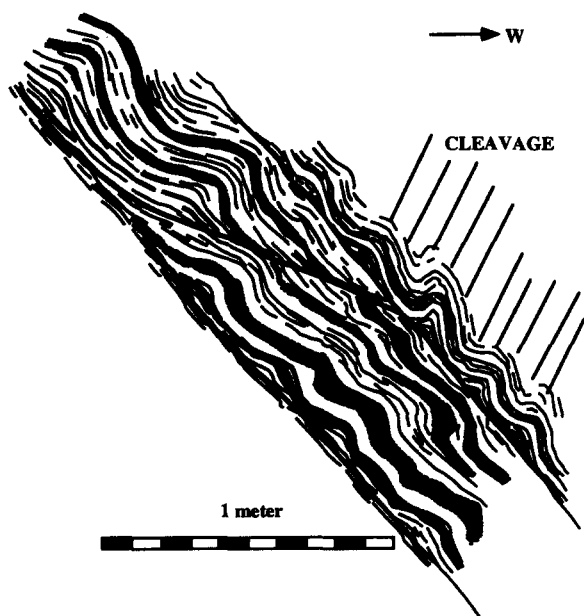


Fig. 10. Small-scale folds from Cacapon Mountain anticlinorium, Wills Creek Formation, with wavelength of centimeters to meters (Geiser personal communication 1992). These folds are not represented in Fig. 4 because of map resolution and are not measured in thin-section scale strain analysis because of their size. Figure 9 predicts that shortening strain from folds like these is around 10%.

sequence has a comparable shortening to that in the underlying blind thrust sheet. This conclusion does not imply that there is no displacement transfer by fore-thrusting; it implies that displacement transferred out is about the same as that transferred in from the internal direction (southeast).

## DISCUSSION

Recognition of fractal strain distribution is important in structural analysis. When performing cross-section modeling and balancing, one must be aware of the map (or cross-section) resolution, since only those structures larger than the resolution limits are presented on the map. Massive competent rock units usually display broad folds and control the structural framework on a large scale. In fractal terminology,  $D$  is close to its topological dimension. In contrast, thin bedded, less competent units, are usually more highly deformed and have a much more complicated geometry. Greater structural detail will be revealed at smaller scales as the resolution of observation is increased, and in this case, the fractal dimension  $D$  is larger than its topological dimension. For these rock units, not only does microscopic strain analysis become important, but outcrop scale observation (the scale between thin section and map scale) is also critical.

Spectral analysis is useful in determining the fractal dimension but has a limited application to geological cross-sections. Many structural profiles have overturned folds, mushroom-shaped folds, thrust faults and/or normal faults. In terms of mathematics, the fold profiles not only have many discontinuities, but they are also not

single-valued. Another problem encountered here is that the spectral fractal dimension is different from the compass fractal dimension even after the profile has been vertically exaggerated. According to Brown (1987), for a self-affine fractal adjusted by an appropriate exaggeration, the compass method should generate a value similar to the spectral method. Whether a special treatment of the raw spectrum is needed should be investigated further.

The compass method is simple and straightforward and can basically be applied to any type of fold profile. Because of limitations when applied to self-affine fractals, however, it must be used with caution since most, if not all, geologic problems are self-affine. An adjustment by exaggerating the vertical direction is necessary when the cross-over length is smaller than the largest ruler used. When the ruler is small, the accumulated error of compass walking becomes very sensitive. A physical problem also exists when a profile is enlarged tens or even hundreds of times in one direction, and a computer program (Brown 1987) is needed to perform the compass walking procedure.

As pointed out by Mandelbrot (1985), a self-affine fractal does not have a global fractal dimension. This is especially true here since geological structures are controlled by many factors. Tectonic processes, basement configuration, rock strength and formation thickness affect the large-scale structural geometry. Deformation mechanisms, rock composition, texture, grain size, strain rate, temperature, pressure and pore fluids affect the small-scale structural geometry. The scaling property apparently changes from one mountain belt to another, and from one province to another within a mountain belt. It is critical to characterize these fractal domains and to find to what limit a fractal dimension applies.

The Cambrian–Ordovician rocks do not crop out in the Cacapon Mountain anticlinorium. Therefore, it is unknown exactly how much small-scale and microscopic strain exists in this stratigraphic interval. The carbonate rocks do crop out about 18 km east of the Cacapon Mountain anticlinorium in the hanging wall of the North Mountain thrust fault and also at the southern terminus of the core of the Adams Run anticlinorium. Cloos (1971) determined the strain axial ratios from oolites in the Cambrian–Ordovician carbonates to be 1.28–1.68 (12–22% layer-parallel shortening). This strain is mainly due to the large displacement of the underlying North Mountain thrust fault. Dean & Kulander (1972) have found that the deformed oolites in the Cambrian–Ordovician carbonates in the immediate vicinity of the North Mountain fault zone commonly have high strain ratios ( $R = 2.6$ ). In the Cacapon Mountain area, the strain in the carbonates should be much smaller (Mitra 1987, Ferrill & Dunne 1989) because the displacement of the Cambrian–Ordovician thrust sheet is much smaller (about 7.25 km) than the 60 km displacement on the North Mountain thrust fault (Kulander & Dean 1986). In their laboratory models, Liu & Dixon (1990) and Dixon & Tirrul (1991) found that both competent

and incompetent units have experienced a significant amount of layer-parallel shortening strain in the early stages of deformation. A 5% layer-parallel shortening could be a reasonable estimation for the carbonates. If this is true in the Cacapon Mountain area, the fractal dimension of the Cambrian–Ordovician carbonates cannot be extrapolated to the finer scale (Fig. 8) because there may be a cross-over length which is very small and cannot be detected by the profile analysis. The general conclusion will not be affected by a few-percent microscopic strain in the carbonates. Because  $D$  in the massive carbonates is still much smaller than  $D$  in the cover units, the two lines (Fig. 9) will intersect. Structural analysis at the resolution indicated by the intersection point will reveal equivalent shortening in both the massive carbonates and the cover units. These arguments need to be tested by sampling from well cores, if available, or from the outcrops in the Adams Run anticlinorium.

### CONCLUSIONS

Strain distribution has a scaling property which can be described appropriately by a fractal dimension  $D$ . A value of  $D$  close to one means that not much strain is accommodated by small-scale structures. If  $D$  is significantly larger than 1, it means that a significant amount of strain is accommodated by structures at smaller scales. When balancing a cross-section, one must consider shortenings at all scales for those units with  $D > 1$ .

Most geological features of fractal geometry are self-affine. When a compass method is used to estimate the fractal dimension, one must make sure that the maximum ruler used is much smaller than the cross-over length. A proper treatment by vertically exaggerating the profile is necessary when the cross-over length is small.

A fractal strain distribution in the Cacapon Mountain anticlinorium argues that the shortening in the cover sequence is comparable with that in the underlying blind Cambrian–Ordovician carbonate thrust sheet when strains from thin section scale through outcrop scale to map scale are all included.

*Acknowledgements*—Richard H. Groshong, Jr and William A. Thomas have reviewed the manuscript and discussed a critical point about fractal strain distribution. Careful reviews by David A. Ferrill, Stuart L. Dean and Mark Rowan have greatly improved the manuscript, although David A. Ferrill may disagree with certain aspects. I would also like to thank my wife Weiping L. Wu for her support during this work.

### REFERENCES

- Aviles, C. A., Scholz, C. H. & Boatwright, J. 1987. Fractal analysis applied to characteristic segments of the San Andreas fault. *J. geophys. Res.* **92**, 331–344.
- Brown, S. R. 1987. A note on the description of surface roughness using fractal dimension. *Geophys. Res. Lett.* **14**, 1095–1098.
- Brown, S. R. & Scholz, C. H. 1985. Broad bandwidth study of the topography of natural rock surfaces. *J. geophys. Res.* **90**, 12,575–12,582.
- Cardwell, P. H., Erwin, R. B. & Woodward, H. P. 1968. Geologic map of West Virginia (1:250,000). West Virginia Geological and Economic Survey Publication WV 1, Morgantown, West Virginia.
- Chatfield, C. 1984. *The Analysis of Time Series: An Introduction*. Chapman & Hall, New York.
- Cloos, E. 1971. *Microtectonics along the Western Edge of the Blue Ridge, Maryland and Virginia*. Johns Hopkins University Press, Baltimore.
- Dean, S. L. & Kulander, B. R. 1972. Oolite deformation associated with faulting in the northern Shenandoah Valley. In: *Appalachian Structures, Origin, Evolution and Possible Potential for New Exploration Frontiers* (edited by Lessing, P., Hayhurst, R. I., Barlow, J. A. & Woodfork, L. D.). West Virginia Geological and Economic Survey, Morgantown, West Virginia, 103–139.
- Dean, S. L., Kulander, B. R. & Lessing, P. 1985. Geology of the Capon Springs, Mountain Falls, Wardensville, Woodstock and Yellow Springs Quadrangles, Hampshire and Hardy Counties, West Virginia. West Virginia Geological and Economic Survey Publication WV-26, Morgantown, West Virginia.
- Dixon, J. M. & Tirrul, R. 1991. Centrifuge modeling of fold thrust structures in a tripartite stratigraphic succession. *J. Struct. Geol.* **13**, 3–20.
- Falconer, K. 1990. *Fractal Geometry, Mathematical Foundations and Applications*. John Wiley & Sons, Chichester.
- Ferrill, D. A. 1987. Analysis of shortening across Cacapon Mountain anticlinorium in the central Appalachians of West Virginia. Unpublished M.S. thesis, West Virginia University, Morgantown, West Virginia.
- Ferrill, D. A. & Dunne, W. M. 1989. Cover deformation above a blind duplex: an example from West Virginia. *J. Struct. Geol.* **11**, 421–431.
- Fox, C. G. 1989. Empirically derived relationships between fractal dimension and power law form frequency spectra. *Pure & Appl. Geophys.* **131**, 211–239.
- Fox, C. G. & Hayes, D. E. 1985. Quantitative methods for analyzing the roughness of the sea floor. *Rev. Geophys.* **23**, 1–48.
- Geiser, P. A. 1974. Cleavage in some sedimentary rocks of the Valley and Ridge Province, Maryland. *Bull. geol. Soc. Am.* **85**, 1399–1412.
- Geiser, P. A. 1988. The role of kinematics in the construction and analysis of geological cross sections in deformed terranes. *Spec. Pap. geol. Soc. Am.* **222**, 47–76.
- Gwinn, V. E. 1964. Thin skinned tectonics in the plateau and north-western Valley and Ridge provinces of the central Appalachians. *Bull. Am. Ass. Petrol. Geol.* **75**, 863–900.
- Hough, S. E. 1989. On the use of spectral methods for the determination of fractal dimension. *Geophys. Res. Lett.* **16**, 673–676.
- Jacobein, F., Jr & Kaness, W. H. 1974. Structure of the Broadtop synclinorium and its implications for Appalachian structural style. *Bull. Am. Ass. Petrol. Geol.* **58**, 362–375.
- Jenkins, G. M. & Watts, D. G. 1968. *Spectral Analysis and its Applications*. Holden Day, San Francisco.
- Kulander, B. R. & Dean, S. L. 1986. Structure and tectonics of central and southern Appalachian Valley and Ridge and plateau provinces West Virginia and Virginia. *Bull. Am. Ass. Petrol. Geol.* **70**, 1674–1684.
- Liu, S. & Dixon, J. M. 1990. Centrifuge modeling of thrust faulting: strain partitioning and sequence of thrusting in duplex structures. In: *Deformation Mechanisms, Rheology and Tectonics* (edited by Knipe, R. J. & Rutter, E. H.). *Spec. Publ. geol. Soc. Lond.* **54**, 431–444.
- Mandelbrot, B. B. 1967. How long is the coast of Britain? Statistical self similarity and fractional dimension. *Science* **145**, 636–638.
- Mandelbrot, B. B. 1983. *The Fractal Geometry of Nature*. Freeman, New York.
- Mandelbrot, B. B. 1985. Self-affine fractals and fractal dimension. *Physica Scripta* **32**, 257–260.
- Mandelbrot, B. B., Passoja, D. E. & Paullay, A. 1984. Fractal character of fracture surfaces of metals. *Nature* **308**, 721–722.
- Mitra, S. 1986. Duplex structures and imbricate thrust systems: Geometry, structural position, and hydrocarbon potential. *Bull. Am. Ass. Petrol. Geol.* **70**, 1087–1112.
- Mitra, S. 1987. Regional variations in deformation mechanisms and structural styles in central Appalachian orogenic belt. *Bull. geol. Soc. Am.* **98**, 569–590.
- Okubo, P. G. & Aki, K. 1987. Fractal geometry in the San Andreas fault system. *J. geophys. Res.* **92**, 345–355.
- Perry, W. J., Jr. 1978. Sequential deformation in the central Appalachians. *Am. J. Sci.* **278**, 518–542.
- Power, W. L. & Tullis, T. E. 1991. Euclidean and fractal models for the description of rock surface roughness. *J. geophys. Res.* **96**, 415–424.

- Rogers, J. 1963. Mechanics of Appalachian foreland folding in Pennsylvanian and West Virginia. *Bull. Am. Ass. Petrol. Geol.* **74**, 1527–1536.
- Turcotte, D. L. 1989. Fractals in geology and geophysics. *Pure & Appl. Geophys.* **131**, 171–196.
- Turcotte, D. L. 1991. Fractals in geology: what are they and what are they good for? *GSA Today* **1**, 1–4.
- Wilson, T. H. 1988. The Fourier analysis of structural cross section. *Comput. Orient. geol. Soc. Comput. Contr.* **4**, 56–78.
- Wilson, T. H. & Shumaker, R. C. 1988. Three dimensional structural interrelationships within Cambrian Ordovician lithotectonic unit of central Appalachians. *Bull. Am. Ass. Petrol. Geol.* **72**, 600–614.
- Wong, P. 1987. Fractal surfaces in porous media. *Am. Inst. Phys. Con. Proc.* **154**, 304–318.
- Wong, P., Howard, J. & Lin, J. 1986. Surface roughening and fractal nature of rocks. *Phys. Rev. Lett.* **57**, 637–640.
- Woodward, N. B., Gray, D. R. & Spears, D. B. 1986. Including strain in balanced cross-sections. *J. Struct. Geol.* **8**, 313–324.